Article **Journal of Research and Development**
June 2023, Vol.9 No.23 1-9

Numerical modeling of the behavior of a lithium battery after a collision

Modelado numérico del comportamiento de una batería de litio tras colisión

FLORES-LÓPEZ, Holbein Eli†*, LÓPEZ-GARCÍA, Claudio and SANTIAGO-AMAYA, Jorge

Instituto Politécnico Nacional, Escuela Superior de Ingeniería Mecánica y Eléctrica Unidad Zacatenco. Maestría en Ciencias en Ingeniería Mecánica, C.P. 07738 Ciudad de México, México.

ID 1st Author: *Holbein Eli, Flores-López* / **ORC ID:** 0009-0007-8793-7021 **CVU CONACYT ID:** 1141571

ID 1st Co-author: *Claudio, López-García* / **ORC ID:** 0000-0002-8361-8249 **CVU CONACYT ID:** 333862

ID 2nd Co-author: *Jorge, Santiago-Amaya* / **ORC ID:** 0000-0003-3432-4305, **CVU CONACYT ID:** 490214

DOI: 10.35429/JRD.2023.23.9.1.9 Received: January 10, 2023; Accepted: June 30, 2023

Abstract

This study is carried out to verify numerically the deformation and Von Misses stresses of a lithium-Ion battery (Li6PF 43 ah, 3.7v) after impact against a solid sphere, using the specialized program in Dynamic Simulation. and Ls-Dyna Finite Elements. With the aim of advancing in the studies to validate the safety of batteries in electric cars this study creates a model of the analyzed prismatic battery.

Battery, Finite element, Lithium, Simulation

Resumen

Se realiza este estudio con el fin de comprobar numéricamente la deformación y los esfuerzos de Von Misses de una batería de Ion de litio, (Li6PF 43 ah, 3.7v) tras el impacto contra una esfera sólida, haciendo uso del programa especializado en Simulación Dinámica y Elementos Finitos Ls-Dyna. Con el objetivo de avanzar en los estudios para validar la seguridad de baterías en automóviles eléctricos, este estudio crea un modelo propio de la batería prismática analizada.

Batería, Elementos finitos, Litio, Simulación

Citation: FLORES-LÓPEZ, Holbein Eli, LÓPEZ-GARCÍA, Claudio and SANTIAGO-AMAYA, Jorge. Numerical modeling of the behavior of a lithium battery after a collision. Journal of Research and Development. 2023. 9-23:1-9.

* Author's Correspondence (E-mail: holbeineli@gmail.com)
† Researcher contributing as first author.

Introduction

With the advent of lithium-ion battery technology, hybrid or fully electric cars have become popular on the world's roads. With the advent of this type of transport, new safety protocols had to be implemented in case of serious accidents (Electric Cars Are Triggering New Emergency Protocols Due to Batteries and Their Fire Hazards, n.d.; NFPA, n.d.).

Cases of accidents involving problems with electric vehicle batteries have been reported (Beauregard et al., 2008)(U.S. Department of Transportation, 2012)(Feng et al., 2018). These are caused by several reasons, one of which is mechanical abuse, which includes deformation and displacements, caused by forces applied during a collision, which would result in battery pack deformation, separator rupture causing short circuits and leakage of flammable electrolyte (Feng et al., 2018).

With existing technology, aspects of vehicle safety can be analysed, such as software simulation, where the behaviour of a battery bank can be analysed after a sudden impact and under specific circumstances.

In a study conducted at the Department of Mechanical Engineering at Ningb University of Technology in China (Chen et al., 2020), a solid sphere is impacted on a lithium battery, resulting in stresses and a marked footprint on the battery. The data obtained are corroborated by performing a numerical analysis using the finite element program Ls-Dyna, by running a simulation to observe the Von Misses stresses, in such a way that it contributes to express results in a numerical way.

Distortion energy

The strain energy of an element is the increase in energy associated with the deformation of the element. During a tensile test, the elongation of a specimen under the action of an increasing load is measured, work is expended and this work is partially or totally transformed into potential strain energy. If the deformation does not reach the elastic limit, the work done by the external force is completely transformed into potential energy and can be recovered by gradually unloading the deformed bar (STEPHEN P. TIMOSHENKO, 1972).

The strain energy density of a material is the strain energy per unit volume, which is equal to the area under the stress-strain curve.

$$U = \int_0^{x_1} P dx \tag{1}$$

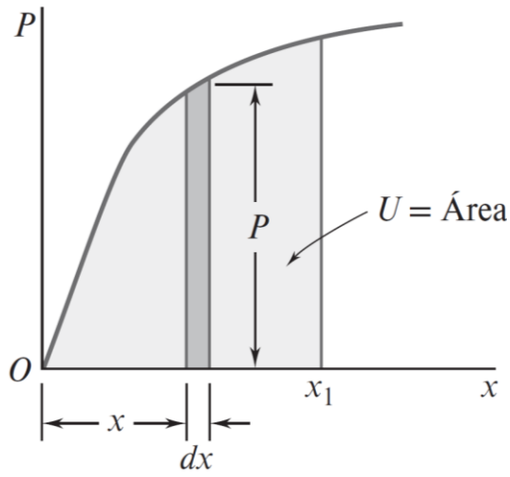

Figure 1 Stress-Strain graph

Strain energy can be used to determine the effects of impact loads on structures or machine components. For practical purposes, equations 2 and 3 are given, in which the strain energy as a function of geometric, elastic and load characteristics, and in another is expressed as a function of the same characteristics and the elongation, respectively.

$$U = \frac{Pl}{AE} \tag{2}$$

$$U = \frac{Pl}{AE} \tag{3}$$

The theory states that: "Failure will occur when the distortion energy per unit volume due to the absolute maximum stresses at the critical point is equal to or greater than the distortion energy per unit volume of a specimen in the tensile test at the time of creep" (FERDINAND P. BEER, 2015).

This criterion determines the distortion energy in a material, which is the energy associated with changes in the shape of the material. It is also known as the Von Mises criterion. A component is safe as long as the maximum value of the distortion energy per unit volume in that material remains smaller than the distortion energy per unit volume required to yield a specimen of the same material under stress.

The equivalent stress is given by:

ISSN-On line: 2444-4987

$$\sigma_{eq} = \sqrt{\frac{1}{2}[(\sigma_1 - \sigma_2)^2 + (\sigma_2 - \sigma_3)^2 + (\sigma_3 - \sigma_1)^2]} \quad (4)$$

Comparing the graph given by Von Misses against that of Tresca, the Von Misses graph being the ellipse and the Tresca graph being the hexagon formed; it establishes the allowable stress values to achieve design reliability of materials.

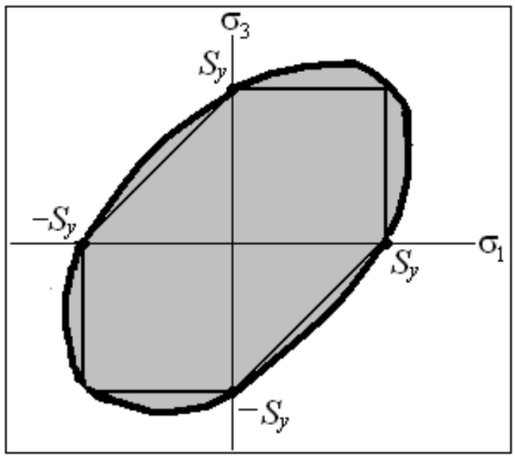

Figure 2 Von Misses vs Tresca chart

Ls-Dyna

Ls-Dyna is a multiphysics simulation program capable of simulating complex problems. It uses a general finite element code for the extensive analysis of static and dynamic deformations of structures, including fluid-coupled structures. The main solution methodology used by this application is based on an explicit integration time. A contact-impact algorithm allows difficult contact problems to be easily treated with heat transfer including interface contact.

Ls-Dyna currently contains approximately 1000 constitutive models and 10 equations to cover a wide range of material behaviour.

Originated at Lawrence Livermore National Laboratory, the first application was for the analysis of stresses in structures subjected to various impact loads. The application required certain computational resources, and the need for a much faster version was necessary, as the results took a long time to appear, all in accordance with the technology at the time.

It is widely used in the automotive industry for the design and development of projects involving the improvement and safety of its occupants, as well as in the study of metal deformation. On the other hand, in the aerospace industry it is used in the study of materials and the prevention of structural errors in new designs. It is also being used for non-linear materials that do not exhibit ideally elastic behaviour.

It consists of a single executable file and uses line-driven commands. Therefore, all that is required to run Ls-Dyna is a command console, the executable, an input file and enough free disk space to run the calculation. All input files are in ASCII format, although it can run various types of files dealing with CAD design (STL) and can therefore be prepared using any text editor. Input files can also be prepared with the help of a graphics preprocessor.

Ls-Dyna is one of the most popular Code-based explicit finite element solvers used for structural simulation when subjected to dynamic loads. The program is used in industry for the design and prediction of various structures ranging from automobiles to aircraft components when subjected to shock or impact loads (JOHN O. HALLQUIST, 2006).

Battery design

Li-ion batteries have a high energy density, good high temperature performance and are recyclable. The main advantages of Li-ion batteries are low memory effect, high specific power (W/kg), high specific energy (Wh/kg) and long life. These characteristics make these batteries suitable for use in hybrid electric vehicles and electric vehicles (Iglesias et al., 2012).

On the downside, due to the nature of the chemical reactions of lithium, these batteries are not tolerant of overcharging or over-discharging and can easily be damaged if the control strategy is inadequate, making safety an added issue. Commercial Li-ion batteries often have protection systems built into the battery body itself to limit charging voltages, discharge voltages and disconnect cells from the load in the event of overcurrent or overtemperature (Wang et al., 2019).

ISSN-On line: 2444-4987

Impact testing

Zhang developed a finite element model, a battery separator in Ls-Dyna. Based on uniaxial tensile and full-thickness compression test data. The model allowed to obtain the response of the separator under drilling tests with different drill head sizes. The model also correctly responded to the effect of anisotropic material on the shape and curvature of the deformation in two planes of anisotropy figure 3 (Zhang *et al*., 2016).

Figure 3 Indentation with different sphere sizes

Meng L. performed a nail penetration test to observe the behaviour of a lithium battery. The cell chosen is a commercial hard-shell prismatic lithium-ion cell with a rated capacity of 202 Ah. The test was performed with the lithium cell encapsulated with a silicon base, inside a thick-walled metal enclosure. The encapsulation technique was devised and designed to ensure that, once the cell is vented, the encapsulation at the vent perimeter would also break down without damaging the adjacent encapsulation. Figure 4 shows the nail penetration test to the metal enclosure containing the silicon-encapsulated battery and a general schematic of the test.

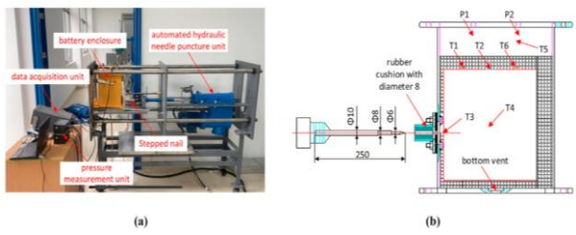

Figure 4 a) penetration test set up. b) penetration test schematic

A second penetration test was performed, only this time more batteries connected in series were used. What happened this time was that the efficiency of encapsulating the batteries with silicone is tested, since, in case of leakage, the silicone material keeps the other batteries and their terminals isolated (Meng et al., 2022). From the studies with the encapsulation method, Lingyu recorded data showing that the technique really works to dissipate heat, figure 5.

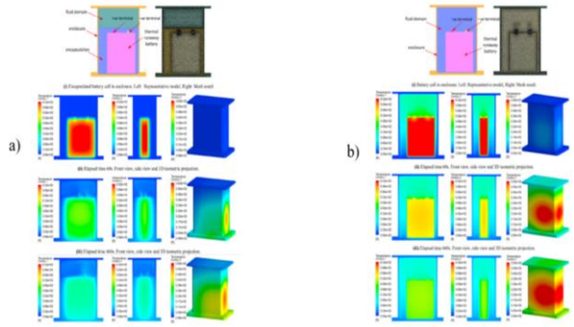

Figure 5 a) Temperature distribution with the encapsulation technique. b) Temperature distribution without encapsulation

Another research paper, Lars Greve and Clemens Fehrenbach, discuss the safety of lithium-ion battery cells, and talk about two general strategies that can be applied to safety; the first is to improve safety by avoiding overuse and protecting the cells adequately; the second is to improve cell safety by understanding the mechanisms that cause internal short circuits under mechanical load and improving cells or cell components accordingly. In their study they perform mechanical tests with cylindrical lithium-ion cells. The simulation model allows the representation of cell deformation and a tensile-based fracture criterion to predict the state of charge and the location of internal short-circuit initiation during deformation. I conducted quasi-static tests, which showed that the cells could withstand significant deformation before a short circuit could occur (Greve & Fehrenbach, 2012).

With a force of less than .2 KN. A punch velocity of .5 mm/ms and an actual test velocity of .1 mm/s it is proposed as future work to involve experimental characterisation and numerical simulation of the individual components of the gelatin roll (anode, separator and cathode) and their interaction during mechanical loading. [9]

Karen Dai, He Zhang and Zheng You used the machete hammer test, which converts the kinetic energy of a hammer's counterweight into gravitational potential energy. They performed impact tests on a lithium-ion battery. During the tests they monitored the voltage behaviour of the battery. The results obtained show a significant change in voltage during impact. Another result was to measure internally the deceleration at the time of an embedding, by means of the oscillation at the time of vibration caused by the generated stress waves.

ISSN-On line: 2444-4987

The impact circuit model presented in this paper can analyse the failure behaviour under high-speed impact, but cannot reveal structural parameters of lithium-ion batteries in impact resistance. They propose an increase of separator thickness which significantly improves the failure phenomenon of lithium-ion batteries under high impact (Yu et al., 2021).

Methodology

For this work, the case study of a prismatic battery indentation from a thesis study (Chen et al., 2020) will be replicated numerically. This experiment consists of a drop-weight impact test system (model: DHR-1808) to impact a prismatic battery. A spherical indenter was used. The impact velocity was varied from 1.5 m/s to 4.5 m/s increasing by .25 to .25 and .5 m/s. A total of 8 indentations were performed. What will be reproduced is only the moment of impact to the battery, without taking into account the test machine, only the battery and the indenter.

With the data provided, we proceeded with the numerical simulation replica using the Ls-Dyna programme for the battery impact test. The steps necessary to arrive at the final result will be explained, and from this we will compare the data obtained with the experiment of the thesis on which this work is based.

Block diagram of the methodology

BLOCK 1
The battery was disassembled to examine its internal components and obtain the necessary measurements to recreate its CAD model.

↓

BLOCK 2
With the measurements obtained of the internal components of the battery, we proceeded to draw and recreate each essential part of the battery in CAD.

↓

BLOCK 3
With the 3 essential parts of the battery an assembly was made to obtain the CAD model of the battery.

↓

BLOCK 4
The CAD model was saved in IGES format and opened in the dynamic simulation program Ls-Dyna.

↓

BLOCK 5
The Ls-Dyna program cards were programmed with the necessary boundary conditions and the essential materials to recreate the moment of impact of the battery with the half-sphere indenter and observe if the behaviour of the battery is the same, similar or different to the experimental case study being evaluated in this work.

↓

BLOCK 6
With the Ls-Dyna cards correctly programmed, we proceeded to run the simulation.

The following figure shows the finished CAD model, the design program used was SolidWorks.

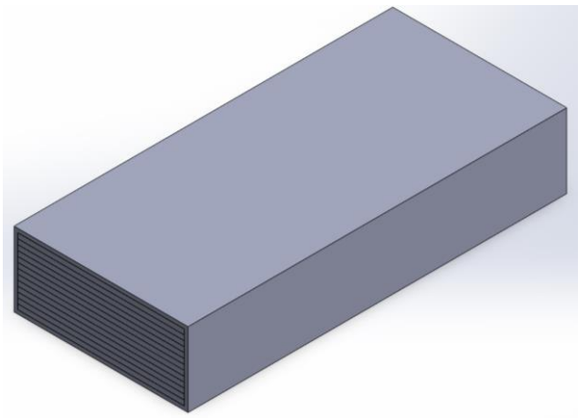

Figure 6

Once the CAD model design step was completed, the next step was to use the Ls-Dyna program for the simulation of the battery impact. The SolidWorks file with extension .igs was used and loaded into the Ls-Dyna program. The following figure shows all the components ready and meshed for simulation.

ISSN-On line: 2444-4987

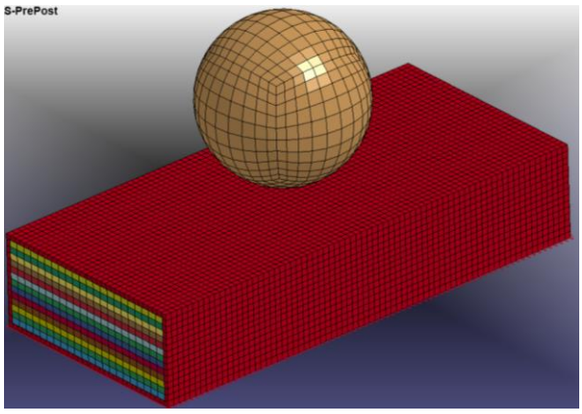

Figure 7

As can be seen in the figure, the model was trimmed at the ends to optimise and reduce computational costs. It is considered that the results do not vary much due to the eliminated parts of the rounded edges.

The cards that were used for preprocessing and simulation are presented below.

First, the materials were added with their corresponding densities, Young's modulus, Poisson's ratio and yield stress.

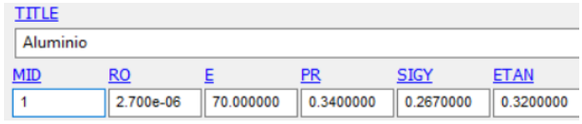

Figure 8 Mat 003 Plastic Kinematic (Aluminum)

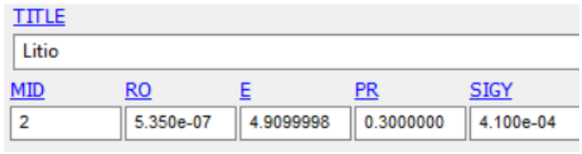

Figure 9 Mat 003 Plastic Kinematic (Litio)

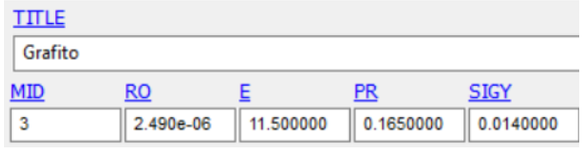

Figure 10 Mat 003 Plastic Kinematic (Graphite)

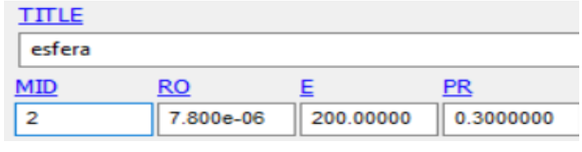

Figure 11 Mat 020 Rigid, material for the sphere (Steel)

Then 2 sections are created, one for each type of solid that integrates the model. The battery casing will be taken as a Shell, as this is the mesh that was assigned to it by the program tools. For the sphere and the other parts of the battery, it will be taken as a Solid, since the programme tools allowed a solid mesh for these parts.

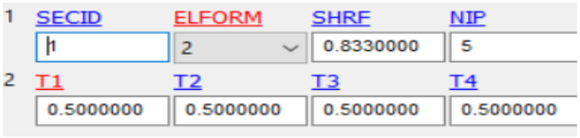

Figure 12 Shell section with a thickness of .5 mm

Figure 13 Solid Section, the card is created without adding anything

The next step is to create a Part to assign a material and a section to each Part in the simulation, in this case we have 15 parts to which we need to add a material and a section.

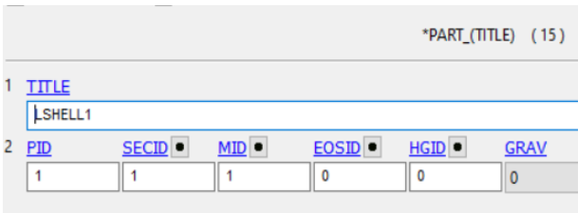

Figure 14 Part 1 with SECID as section and MID as material

For each component a section and material needs to be assigned as appropriate, for this case components 2 to 15 will be assigned a Solid section corresponding to their mesh type and the housing will be assigned a Shell section due to its assigned mesh type. The sphere will be assigned to the steel material and the shell to aluminium, all others will be sandwiched between graphite and lithium.

We assign a negative velocity on the y-axis to the sphere.

Figure 15 In NSID/PID select the desired item to be assigned a speed

ISSN-On line: 2444-4987

A motion constraint is programmed to make the battery stand still, simulating the test table where it is located, using the SPC_SET board, as shown in Figure 17.

Figure 17 The section of nodes created is chosen

When it comes to choosing a node section, it will ask us to create it, so we create it on the entire bottom side, as shown in Figure 17.

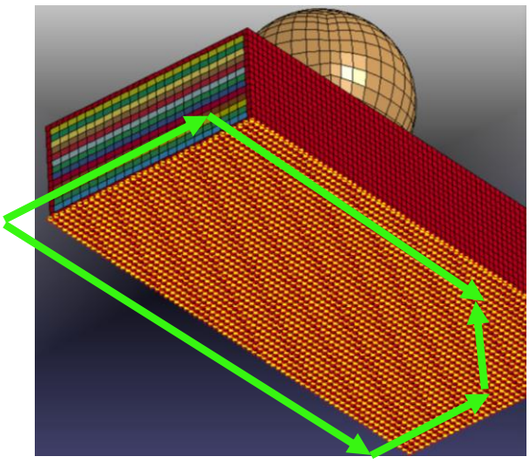

Figure 18 Movement restriction using SET_NODE (marked with green colour)

We continue with filling the cards of the types of contacts that will occur in the simulation. Taking into account that the sphere is the master and where it hits is the slave, we fill the fields with the necessary parts. After the first contact of the sphere against the first layer of the battery, the same logic is followed to determine who is now the master and who is the slave. As shown in Figures 18-32.

Figure 19 Contact1

Figure 20 Contact 2

Figure 21 Contact 3

Figure 22 Contact 4

Figure 23 Contact 5

Figure 24 Contact 6

Figure 25 Contact 7

Figure 26 Contact 8

Figure 27 Contact 9

Figure 28 Contact 10

Figure 29 Contact 11

Figure 30 Contact 12

Figure 31 Contact 13

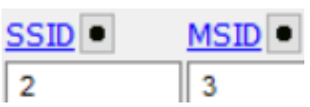

Figure 32 Contact 14

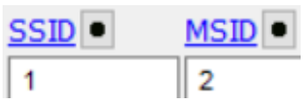

Figure 33 Contact 15

Finally, we set the time we want the simulation to last, we do it at 1 ms Figure 33.

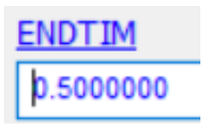

Figure 34 Control_Termination card

We must also give a time in which we want the program to make measurements of the results, and we will set it to .01, Figure 34.

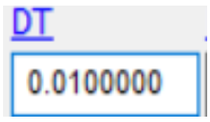

Figure 35 Binary D3plot card

We save our .k file and solve it with the Ls-Dyna solver, when finished we can open the D3plot file that it generates and that is the file to visualize the results.

We also achieve what we expected, to reduce the computational costs with the simplification of the design, as previously explained in Figure 35.

```
estimated total cpu time          =      2250 sec
estimated cpu time to complete    =      2248 sec
estimated total clock time        =      3426 sec
estimated clock time to complete  =      3424 sec
```

Figure 36 Simulation times

Results

Table III.3 shows the results of the simulation with a sphere velocity of 2 m/s. Table 1 shows a comparison of the experimentally obtained results against the simulation results in Ls-Dyna.

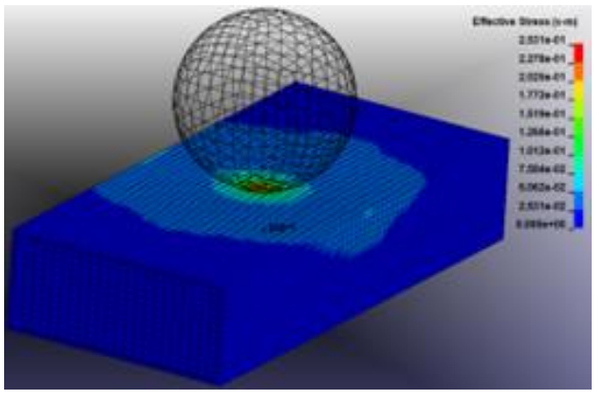

Figure 37 Battery impact zone: Time: 1.9998 m/s Von Misses Maximum Stress = .2531 Pa

Time: 1.9998 m/s Von Misses Maximum Stress =.2531Pa

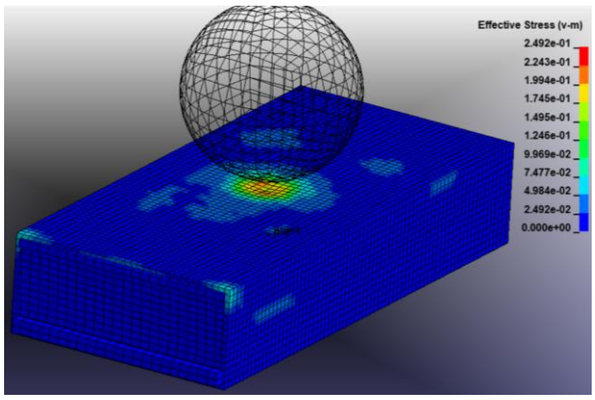

Figure 38 Battery impact zone: Time: 10 m/s Von Misses Maximum Stress = .2492 Pa

Time: 10 m/s Von Misses Maximum Stress= .2492 Pa

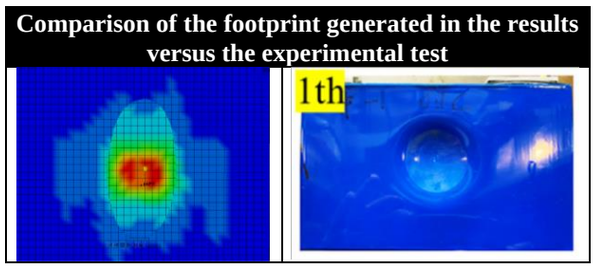

Table 1 Comparison of the generated footprint.

Acknowledgements

I thank the Doctors who supported me so that it was possible to finish writing this article. I thank my family for supporting me and allowing me to continue to achieve my goals, especially my parents because they gave me their support so that I could follow this path of knowledge.

ISSN-On line: 2444-4987

Conclusions

The deformations resulting from the numerical simulation are congruent with those presented experimentally. Deformations that are at low speeds but that manage to deform the battery, which will affect the correct operation of a battery of these characteristics.

The lithium-ion battery studied in this work presents conditions of easy deformation. Therefore, the necessary precautions must be taken for its use under the load conditions presented.

References

Beauregard, Garret P., & Phoenix. (2008). *Informe de Investigación: Híbridos más vehículo hibrido eléctrico enchufable.*

Chen, X., Yuan, Q., Wang, T., Ji, H., Ji, Y., Li, L., & Liu, Y. (2020). Experimental study on the dynamic behavior of prismatic lithium-ion battery upon repeated impact. *Engineering Failure Analysis*, *115*, 104667. https://doi.org/10.1016/j.engfailanal.2020.104667

Departamento de Transporte de EE. UU. (2012). *Informa general de incidentes de batería de voltios de Chevrolet*.

Feng, X., Ouyang, M., Liu, X., Lu, L., Xia, Y., & He, X. (2018). Thermal runaway mechanism of lithium ion battery for electric vehicles: A review. *Energy Storage Materials*, *10*, 246–267. https://doi.org/10.1016/J.ENSM.2017.05.013

FERDINAND P. BEER. (2015). *MECÁNICA DE MATERIALES* (E. RUSSELL JOHNSTON, DEWOLF T., & MAZUREK F. DAVID, Eds.; SÉPTIMA EDICIÓN). Mc Graw Hill.

Greve, L., & Fehrenbach, C. (2012). Mechanical testing and macro-mechanical finite element simulation of the deformation, fracture, and short circuit initiation of cylindrical Lithium ion battery cells. *Journal of Power Sources*, *214*, 377–385. https://doi.org/10.1016/j.jpowsour.2012.04.055

Iglesias, R., Lago, A., Nogueiras, A., Martínez-Peñalver, C., Marcos, J., Quintans, C., & Moure, M. (2012). *Modelado y Simulación de una Batería de Ion-Litio Comercial Multicelda*.

JOHN O. HALLQUIST. (2006). *LS-DYNA THEORY MANUAL* (Livermore Software).

Los coches eléctricos están provocando nuevos protocolos de emergencia debido a las baterías y sus riesgos de incendio. (n.d.). Retrieved May 7, 2023, from https://www.xataka.com/vehiculos/coches-electricos-estan-provocando-nuevos-protocolos-emergencia-debido-baterias-sus-riesgos-incendio

Meng, L., See, K. W., Wang, G., Wang, Y., Zhang, Y., Zang, C., & Xie, B. (2022). Explosion-proof lithium-ion battery pack – In-depth investigation and experimental study on the design criteria. *Energy*, *249*, 123715. https://doi.org/10.1016/j.energy.2022.123715

NFPA. (n.d.). Retrieved May 7, 2023, from https://www.nfpa.org/

STEPHEN P. TIMOSHENKO. (1972). *MECHANICS OF MATERIALS* (GERE J. M., Ed.).

Wang, Q., Mao, B., Stoliarov, S. I., & Sun, J. (2019). A review of lithium ion battery failure mechanisms and fire prevention strategies. *Progress in Energy and Combustion Science*, *73*, 95–131. https://doi.org/10.1016/j.pecs.2019.03.002

Yu, D., Ren, D., Dai, K., Zhang, H., Zhang, J., Yang, B., Ma, S., Wang, X., & You, Z. (2021). Failure mechanism and predictive model of lithium-ion batteries under extremely high transient impact. *Journal of Energy Storage*, *43*, 103191. https://doi.org/10.1016/j.est.2021.103191

Zhang, X., Sahraei, E., & Wang, K. (2016). Deformation and failure characteristics of four types of lithium-ion battery separators. *Journal of Power Sources*, *327*, 693–701. https://doi.org/10.1016/j.jpowsour.2016.07.078

ISSN-On line: 2444-4987